



# African Journal of Biological Sciences



## Towards Accurate Multiclass Skin Disease Classification Using Deep Belief Networks on Color-Texture Features

**Dr. A. Kalaivani**

Assistant Professor, Department of Computer Technology, Nallamuthu Gounder Mahalingam College, Pollachi,  
Coimbatore, Tamil Nadu, India  
kalaivanimathsca@gmail.com

### **ABSTRACT—**

Early and accurate detection of skin diseases is essential for effective treatment. However, there is often a gap between dermatologists and patients due to a lack of knowledge about symptoms and stages of skin conditions. This study introduces an innovative dual deep learning-based classifier for skin disease classification model that aims to bridge this gap using machine learning techniques. The model undergoes various preprocessing steps, such as image resizing, hair removal, and noise reduction, to improve image quality. It then utilizes the Mask Residual Convolutional Neural Network (Mask-RCNN) architecture for instance segmentation to isolate lesion regions in skin images. Color and texture features are extracted from the segmented lesions and input into the proposed Dual Deep Belief Network (DDBN) classifiers for concurrently classifying multiple skin diseases. Experiments conducted on the ISIC 2019 Challenge and HAM10000 datasets demonstrate the DDBN's effectiveness, achieving high accuracy, precision, recall, and F1-score compared to the existing classification models. The DDBN's robust classification capabilities can aid dermatologists and patients in the early detection of skin diseases for timely intervention.

**Keywords—**Skin diseases, Preprocessing, Mask-RCNN, Color features, Texture features, Deep belief network

Article History

Volume 6, Issue 5, 2024

Received: 01 May 2024

Accepted: 09 May 2024

doi:10.33472/AFJBS.6.5.2024.2672-2692

## I. INTRODUCTION

The skin is the largest organ in the human body and any disorder that affects it is known as a skin disease. Skin diseases are highly contagious and can have serious consequences. In 2018, 2794 people in Bangladesh died from skin cancer, and globally, over 14 million cases were diagnosed with 9.6 million deaths [1]. Skin diseases can manifest as changes in color or texture and are caused by viruses, bacteria, allergies, fungal infections, and genetic factors [2]. These diseases primarily affect the outer layer of the skin, known as the epidermis, leading to psychological distress and physical harm [3].

Skin lesions can be categorized into different types, including Actinic Keratosis (AK), Basal Cell Carcinoma (BCC), Benign Keratosis (BKL), Dermatofibroma (DF), Melanoma (MEL), Melanocytic Nevus (NV), Squamous Cell Carcinoma (SCC), and Vascular lesion (VASC) [4]. These lesions vary in symptoms and severity, with some being permanent and others temporary, and may cause pain or be painless. Melanoma is the most dangerous type of skin disease, but early detection can lead to successful recovery in 95% of cases [5]. An automated computer-aided system can help accurately classify skin diseases [6]. There is a significant lack of awareness among the general public about different types, symptoms, and stages of skin diseases, creating a gap between dermatologists and patients. Early detection is crucial for effective treatment, but diagnosing skin diseases accurately can be challenging and costly. The automatic computer-aided system based on machine learning approaches has made it possible to detect the types of skin disease more accurately and quickly [7]. Skin disease classification has been a significant research area for the past three decades, with many studies conducted. Despite numerous research papers on the topic, there is still room for improvement in detection and classification methods. Previous research has focused on single diseases and cannot classify multiple classes effectively. Classifying multiple skin diseases is challenging due to their similar behaviors.

Hence, this study introduces a novel automated classification model for multiple skin diseases. The key contributions of this model include:

- Utilizing preprocessing techniques like image resizing, hair removal, and noise removal to improve skin image quality.

- Employing the Mask-RCNN model to identify and segment lesion regions in skin images without losing any information.
- Extracting color and texture features from the segmented images.
- Developing the DDBN model trained on color and texture features for accurate classification of skin diseases.

The remaining article is organized as follows: Section II covers literature survey. Section III explains the proposed model and Section IV illustrates its efficiency. Section V concludes the study and suggests future enhancements.

## II. LITERATURE SURVEY

Many scholars have proposed different frameworks that combine image processing and machine learning algorithms for classifying various skin diseases. This review examines previous research to understand the procedures used and identify areas for further study.

Hameed et al. [8] developed a multi-class multi-level classification algorithm for identifying various skin diseases. It includes noise removal in pre-processing, a hybrid technique for Region of Interest (ROI) extraction, feature extraction for color and texture, and classification of images. Transfer learning was utilized for deep learning directly from images. However, a limitation was the inconsistency in the dataset due to gathering from various sources. Sinthura et al. [9] developed a skin disease diagnosis model using image processing. They segmented the disease portion using Otsu's method and extracted Gray Level Co-occurrence Matrix (GLCM) features like area, perimeter, mean, and entropy. The Support Vector Machine (SVM) classifier was then used to classify four disease classes: acne, psoriasis, melanoma, and rosacea. However, it was tested on a small dataset with a limited number of features.

Jagdish et al. [10] developed a skin disease detection model using image processing techniques. They utilized fuzzy clustering on a small set of sample images and employed K-Nearest Neighbor (KNN) and SVM classification algorithms with wavelet analysis. It accurately identified the type of skin disease. However, it was tested on a limited number of images with basal and squamous disease classes. Naeem et al. [11] developed a skin cancer prediction model using image processing techniques and SVMs. They applied noise removal and image enhancement techniques, along with the GLCM method to extract image features. The classifier then categorized the images as cancerous or non-cancerous. However, the model's

generalizability was limited by the small dataset. AlDera et al. [12] developed a skin disease diagnosis model using image processing techniques. They used Otsu's method for image segmentation and Gabor, Entropy, and Sobel's techniques for feature extraction on skin images. Classification was done using SVM, random forest, and KNN classifiers, but the accuracies were found to be low.

Hatem [13] developed a system using the KNN classifier to identify and classify skin lesions. However, it was tested on images with normal and benign classes. Maduranga et al. [14] used the MobileNet with transfer learning on the HAM10000 dataset to classify skin diseases. However, it achieved low accuracy. Jain et al. [15] introduced the Optimal Probability-based Deep Neural Network (OP-DNN) for skin disease diagnosis. They pre-processed images, extracted features, and trained the OP-DNN. However, the classification accuracy and sensitivity were not satisfactory. Sreekala et al. [16] developed a hybrid AI-based skin disease classification method using Spectral Centroid Magnitude (SCM) for feature extraction and enhanced CNN for classification. Preprocessing involved using a Median filter to remove noise. However, the accuracy of the method was found to be low.

### III. PROPOSED METHODOLOGY

This section explains the proposed skin diseases classification model in detail. A general block diagram of this study is depicted in Figure 1. The process consists of four main steps: image preprocessing, lesion segmentation, feature extraction, and classification.

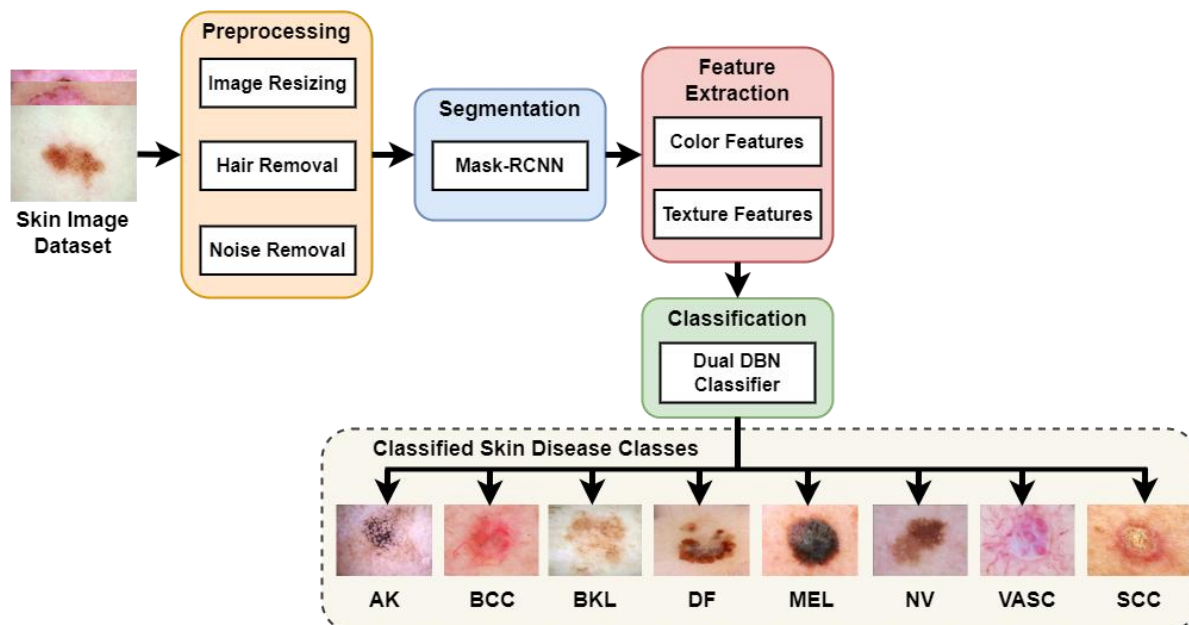


## Figure 1. General Block Diagram of the Proposed Study

### 3.1 Dataset Description

In this study, the following two well-known datasets are considered:

- **ISIC 2019 Challenge Dataset:** The ISIC is an international collection of dermatoscopic images. It combines the HAM10000 and BCN20000 datasets[17]. This study focused on the training dataset of the ISIC 2019 challenge, which includes 25331 dermoscopic pictures of eight different classes: AK, BCC, BKL, DF, MEL, NV, SCC, and VASC.
- **HAM10000 dataset:** This dataset contains 10015 dermatoscopic images of pigmented skin lesions from Australian and Austrian patients [18]. The images are center-cropped to  $600 \times 450$  pixels and belong to seven classes: AK, BCC, BKL, DF, MEL, NV, and VASC.

**Table 1. Distribution of Skin Images in Different Datasets**

Classes	ISIC 2019 Challenge Dataset	HAM10000 Dataset
	Total No. of Images	
<b>BCC</b>	3223	514
<b>AK</b>	867	327
<b>MEL</b>	4522	1113
<b>NV</b>	12875	6705
<b>BKL</b>	2624	1099
<b>DF</b>	239	115
<b>VASC</b>	253	142
<b>SCC</b>	628	-

### 3.2 Preprocessing

Image preprocessing involves converting an image into a more suitable form for use. Skin images often contain unwanted hair, noise, or distortion, which can affect the performance of an image processing system. Preprocessing skin images is essential for improving the performance of skin disease detection systems by enhancing image quality, reducing complexity, and

increasing accuracy. The key preprocessing steps include image resizing, hair removal, and noise removal.

- Image resizing: To ensure consistent feature extraction, images of varying sizes are resized to  $512 \times 512$ . It improves processing time and system performance. An example of skin image resizing is portrayed in Figure 2.



**Figure 2. Example of Skin Image Resizing. (a) Before Resizing and (b) After Resizing**

- Hair removal: Hair removal from images can enhance skin disease detection. A digital hair removal algorithm is used, involving morphological filtering like Black-Hat transformation and inpainting. The steps include converting RGB images to grayscale, applying Black-Hat transformation, creating an inpainting mask, and using the inpainting algorithm on the original image with the mask. An example of hair removal from skin image is portrayed in Figure 3.



**Figure 3. Example of Hair Removal from Skin Image. (a) Before Hair Removal and (b) After Hair Removal**

- Noise removal: Noise can be present in skin images due to various factors such as image acquisition, transmission, and processing. Changes in brightness or color information can also degrade image quality. Gaussian filtering is used to remove noise from the skin images. An example of noise removal from skin image is portrayed in Figure 4.

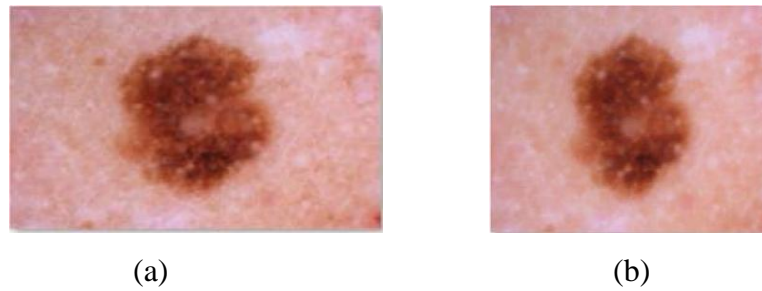
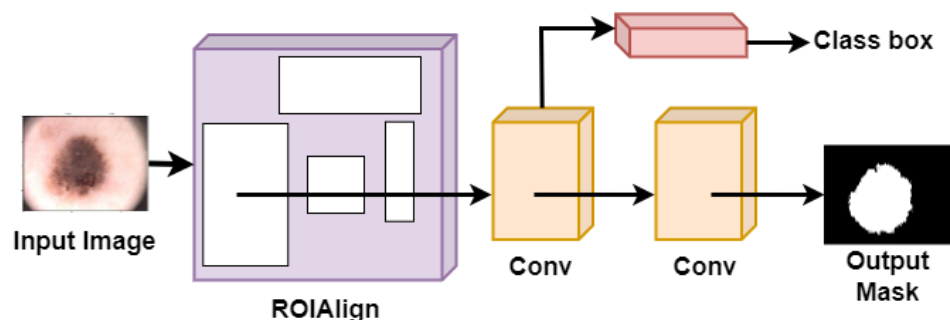


**Figure 4. Example of Noise Removal from Skin Image. (a) Before Noise Removal and (b) After Noise Removal**

### 3.2 Segmentation

Image segmentation is the process of dividing an image into distinct regions based on properties such as gray level, brightness, color, contrast, and texture. This technique is essential for accurately evaluating images, particularly in microscopic images where distinguishing between lesions and healthy skin can be challenging due to variations in size, shape, and color. Accurate segmentation is crucial as it impacts the accuracy of subsequent processes. This study uses the Mask-RCNN model for segmentation.

The lesions are segmented into smaller regions using instance segmentation with Mask-RCNN, which identifies object contours at the pixel level. This step involves processing pre-processed skin images to isolate the cancerous lesions of interest. The Mask-RCNN is an extension of the Faster RCNN model that includes two additional convolutional layers to generate masks. The first stage of the model identifies potential disease locations in the image, while the second stage creates bounding boxes and masks to refine the predictions. ROI alignment is used to align the boundaries of the ROI and scale them to the same dimensions as the input. The feature map values within the areas are calculated using interpolation. The architecture of the Mask-RCNN is illustrated in Figure 5. **Figure 5. Architecture of Mask-RCNN for Skin Image Segmentation**



Mask-RCNN introduces ROI Align, which improves pixel-level segmentation by preserving more spatial information than ROI pooling. Bounding box regression fine-tunes the bounding boxes of the region proposals for a better fit. It predicts segmentation masks at the pixel level for each detected diseased region based on the bounding boxes. Figure 6 shows an example of segmented skin images.



**Figure 6. Example of Skin Image Segmentation. (a) Input Image and (b) Segmented Image**

### 3.3 Feature Extraction

Feature extraction is crucial for analyzing relationships between objects. Image algorithms require feature extraction to convert images into usable forms for tasks like categorization and prediction. Dermoscopic images have various characteristics, but not all are relevant for skin disease classification. Extracting the right features is essential for accurate classification. Using segmented lesion images to extract color and texture features can help determine skin disease type effectively. This study uses mean, standard deviation, skewness, and kurtosis of the green channel pixel values as color characteristics. GLCM are used as texture characteristics. Table 2 provides a summary of the characteristics extracted from the skin images.

**Table 2. Extracted Features from Skin Images**

Type	Features	No. of Features
Color	Color moments	4
Texture	GLCM characteristics	20

**Color Features:** The color moments are a way to represent the color distribution in skin images as a probability distribution. These moments help distinguish skin images based on their color characteristics. There are four sets of color moments: mean color average ( $\mu_C$ ), standard deviation ( $\sigma_C$ ) which defines the distribution region, skewness ( $\theta_C$ ) which describes the color



asymmetry, and kurtosis ( $\gamma_C$ ) which indicates the shape of the distribution curve. These color moments provide valuable information for analyzing and identifying skin images based on their color properties.

$$\mu_C = \frac{1}{WH} \sum_{i=1}^W \sum_{j=1}^H P_{ij}^C \quad (1)$$

$$\sigma_C = \sqrt{\frac{1}{WH} \left( \sum_{i=1}^W \sum_{j=1}^H (P_{ij}^C - \mu_C)^2 \right)} \quad (2)$$

$$\theta_C = \sqrt[3]{\frac{1}{WH} \left( \sum_{i=1}^W \sum_{j=1}^H (P_{ij}^C - \mu_C)^3 \right)} \quad (3)$$

$$\gamma_C = \sqrt[4]{\frac{1}{WH} \left( \sum_{i=1}^W \sum_{j=1}^H (P_{ij}^C - \mu_C)^4 \right)} \quad (4)$$

In Eqns. (1) – (4),  $P_{ij}^C$  is the value of the color element  $C$  (grayscale) on the pixel color of  $i^{th}$  row and  $j^{th}$  column of the skin image,  $W$  and  $H$  denote the width and height of the image, correspondingly.

**Texture Features:**GLCM is derived from grayscale images and is a second-order texture analysis method. Unlike first-order texture analysis, which focuses on statistical estimates of pixel values like variance, GLCM considers the correlation between adjacent pixels. In GLCM, values such as contrast, correlation, energy, and homogeneity are calculated at angles of  $0^\circ$ ,  $45^\circ$ ,  $90^\circ$ , and  $135^\circ$ .

$$Contrast = \sum_{n=0}^{N_g-1} n^2 \left\{ \sum_{i=1}^{N_g} \sum_{j=1}^{N_g} p(i, j) \right\}, |i - j| = n \quad (5)$$

$$Correlation = \frac{\sum_i \sum_j (ij) p(i, j) - (\mu_i \mu_j)}{\sigma_i \sigma_j} \quad (6)$$

$$Energy = \sum_{ij} p(i, j)^2 \quad (7)$$

$$Homogeneity = \sum_i \sum_j \frac{1}{1+(i-j)^2} p(i, j) \quad (8)$$

In Eqns. (5) – (8),  $p(i, j)$  is the distribution of joint probabilities of a pixel pair, one with gray level  $i$  and another with gray level  $j$  and  $N_g$  defines the number of gray levels utilized to create the GLCM. Also,  $\mu_i, \mu_j, \sigma_i$  and  $\sigma_j$  are the mean and standard deviations of the marginal distributions related to  $p(i, j)$  and determined as follows:

$$\mu_i = \sum_{i,j=0}^{N_g-1} i(\mathcal{P}_{i,j}) \quad (9)$$

$$\mu_j = \sum_{i,j=0}^{N_g-1} j(\mathcal{P}_{i,j}) \quad (10)$$

$$\sigma_i = \sum_{i,j=0}^{N_g-1} \mathcal{P}_{i,j} (i - \mu_i) \quad (11)$$

$$\sigma_j = \sum_{i,j=0}^{N_g-1} \mathcal{P}_{i,j} (j - \mu_j) \quad (16)$$

During the feature extraction phase, all the 24 color and texture features of the skin images are obtained, which are then fed to the DDBN classifier.

### 3.4 Classification

In this stage, the DDBN is proposed for skin disease classification. It is a probabilistic network made up of several Restricted Boltzmann Machines (RBMs). There are three layers in the network: output, hidden, and visible. Weights connect the visible and hidden layers, and each neuron has an offset that specifies its weight. To change the key parameters of the hidden layer, the output and the previously hidden layers build a backpropagation neural network. For DBN learning, the input data is taken from the bottom layer and sent to the hidden layers. Figure 7 illustrates the DBN structure with  $n$  hidden layers. The link weights and offsets between the RBM layers are set during pre-learning using an unsupervised greedy layer-by-layer strategy. After that, each RBM layer is individually taught from the bottom to the top.

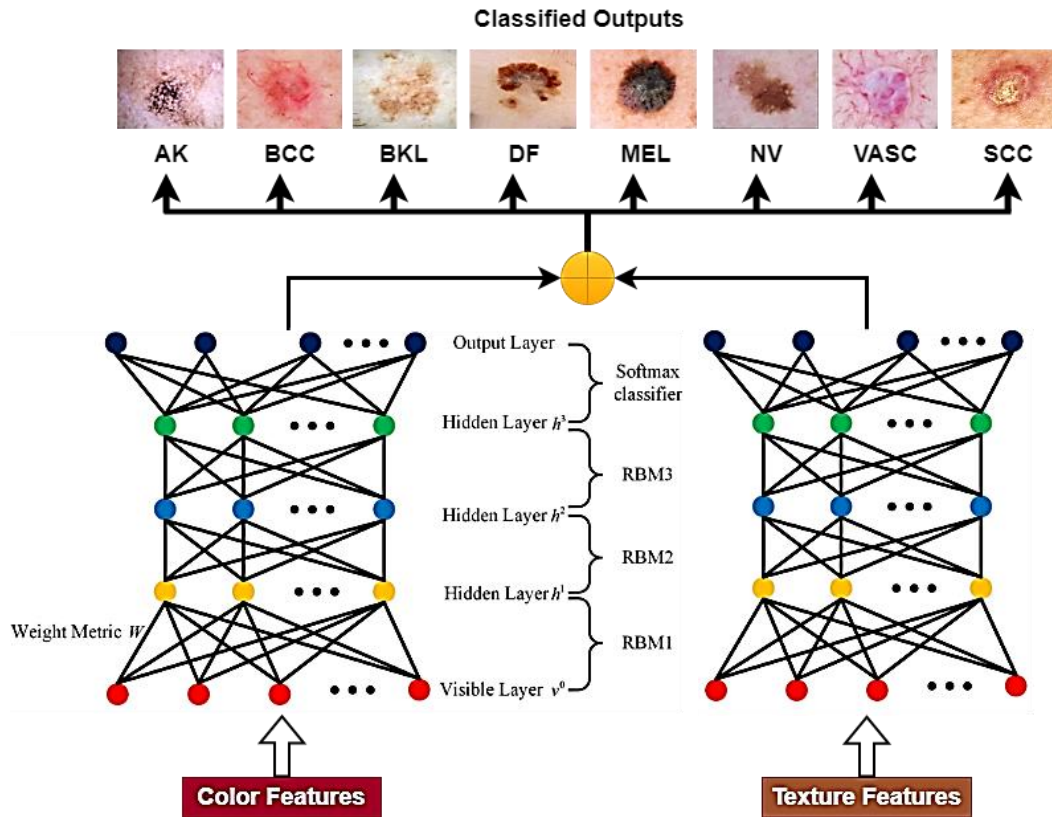


**Figure 7. Architecture of DDBN Model for Skin Diseases Classification**

Let RBM is a power-produced Bernoulli model; the power of the state  $(v, h)$  is as:

$$\begin{cases} E(v, h; \theta) = -\sum_{i=1}^V \sum_{j=1}^H \omega_{ij} v_i h_j - \sum_{i=1}^V b_i v_i - \sum_{j=1}^H a_j h_j, \\ \theta = \{\omega, a, b\} \end{cases} \quad (17)$$

In Eq. (17),  $\theta$  is the RBM parameter,  $\omega_{ij}$  is the link weight between the visible and hidden layer neurons,  $V$  and  $H$  are the number of visible and hidden units,  $v_i$  and  $h_j$  are the node states of the visible and hidden layers,  $b_i$  and  $a_j$  are the offsets of the visible and hidden layers.

To retain sparseness, the visible layer offset  $b_j$  is initialized to  $lb(\hat{p}_i/(1 - \hat{p}_i))$ , where  $\hat{p}_i$  is the chance of  $v_i = 1$ . The hidden layer offset  $a_j$  is initialized to a maximum positive number and  $\omega_{ij}$  is initialized to a minimum arbitrary value. Also, the joint probability of the model is determined as:

$$\begin{cases} P(v, h) = \frac{1}{Z} e^{-E(v, h)}, \\ Z = \sum_{v, h} e^{-E(v, h)} \end{cases} \quad (18)$$

In Eq. (18),  $Z$  denotes the regularization factor. Because there is no link between the peer nodes, the chance of  $v_i$  and  $h_j$  is independent:

$$\begin{cases} p(v_i = 1|h; \theta) = \sigma(\sum_{j=1}^H \omega_{ij} h_j + b_j), \\ P(v_i = 1|h; \theta) = \sigma(\sum_{j=1}^H \omega_{ij} v_i + a_j), \\ \sigma(x) = \frac{1}{1+e^{-x}} \end{cases} \quad (19)$$

In Eq. (19),  $\sigma(x)$  refers to the sigmoid function. The boundary distribution of  $p(v, h; \theta)$  to  $h$  is discovered as:

$$p(v; \theta) = \frac{1}{Z} \sum_h \exp(-E(v, h; \theta)) \quad (20)$$

In Eq. (20),  $\theta$  is obtained by solving the highest log-likelihood prediction function on the training set and the RBM parameter tuning criteria is obtained by the contrast divergence scheme:

$$\begin{cases} \Delta b_i = \varepsilon(\langle v_i \rangle_{data} - \langle v_i \rangle_k), \\ \Delta a_j = \varepsilon(\langle h_j \rangle_{data} - \langle h_j \rangle_k), \\ \Delta \omega_{ij} = \varepsilon(\langle v_i h_j \rangle_{data} - \langle v_i h_j \rangle_k) \end{cases} \quad (21)$$

In Eq. (21),  $\varepsilon$  defines the training efficiency and  $\langle \cdot \rangle_{data}$  and  $\langle \cdot \rangle_k$  are the predicted values of the distribution represented by the present and the reconstructed framework. Because pre-learning is unsupervised training, the primary values of the parameters obtained by pre-learning are not optimum. During this step, the backpropagation neural network is integrated with the label for modifying the parameters for the issue of high outcome error.

The softmax classifier is configured at the output layer of DBN and supervised learning is executed from top to bottom. Based on Eq. (18), the link parameters between all layers are modified to create the best categorization capability of DBN. Thus, multiple DBNs, i.e. two independent DBN for color and texture features, respectively are trained. Their scores are then fused to classify the classes of skin diseases. Table 3 presents the hyperparameters used for constructing the DBN classifier.

**Table 3. Hyperparameters of DBN Model**

Parameters	Range
No. of neurons in input layer	4 (DBN1 for color features) and 20 (DBN2 for texture features)
No. of neurons in RBM1	100
No. of neurons in RBM2	100
No. of neurons in RBM3	100
No. of neurons in output layer	Softmax classifier
Batch size	64
Learning rate	0.001
Momentum value	0.9
Maximum iteration	500

**Algorithm 1:** Pseudocode for Proposed Skin Diseases Classification Model

**Input:** Skin image dataset

**Output:** Classified skin disease labels

1. **Begin**

    //Preprocess input skin images

2. **for**(each image  $I$ )

3. Resize  $I$  to  $512 \times 512$  pixels;

4. Apply hair removal algorithm;

5. Apply noise removal using Gaussian filtering;

6. **end for**

7. Split dataset into training and testing sets;

    //Segment lesions using Mask-RCNN

8. **for**(each preprocessed image  $I$ )

9. Obtain instance segmentation masks  $M$  using Mask-RCNN;

10. Extract segmented lesion regions  $L$  using  $M$ ;

11. **end for**  
    //Extract color and texture features
12. **for**(*each segmented lesion L*)
13. Compute color features (mean, std, skewness, kurtosis);
14. Compute GLCM texture features;
15. **end for**  
    //Train the DDBN model
16. **for**(*color features*)
17. Initialize DBN with RBMs and backpropagation net;
18. Pre-train DBN in unsupervised layer-wise manner;
19. Fine-tune with backpropagation using labeled data;
20. Obtain classification scores  $S_{color}$ ;
21. **end for**
22. **for**(*texture features*)
23. Initialize DBN with RBMs and backpropagation net;
24. Pre-train DBN in unsupervised layer-wise manner;
25. Fine-tune with backpropagation using labeled data;
26. Obtain classification scores  $S_{texture}$ ;
27. **end for**
28. Combine scores:  $S = S_{color} + S_{texture}$ ;  
    //Validate the trained model using the test dataset
29. **for**(*each test image*)
30. Obtain segmented lesion;
31. Compute color and texture features;
32. Obtain  $S_{color}$  and  $S_{texture}$  from trained DBNs;
33. Combine scores  $S = S_{color} + S_{texture}$ ;
34. Predict disease class label using maximum  $S$ ;
35. **end for**
36. **End**

#### IV. EXPERIMENTAL RESULTS

This section assesses the performance of the DDBN model in comparison to existing models such as SVM [9], KNN [13] and OP-DNN [15]. The experimental results were obtained by implementing all models using Python code and testing them with the skin image datasets discussed in Section 3.1. The experiments are conducted on a system with an Intel® Core™ i5-4210 CPU @ 3GHz, 4GB RAM, and a 1TB HDD running on Windows 10 64-bit. The evaluation metrics used to measure the performance improvement include:

- Accuracy: It is the proportion of exact prediction over the total data analyzed.

$$Accuracy = \frac{True\ Positive\ (TP) + True\ Negative\ (TN)}{TP + TN + False\ Positive\ (FP) + False\ Negative\ (FN)} \quad (22)$$

In Eq. (22), TP is the number of positive labels correctly classified as positive, TN is the number of negative labels correctly classified as negative, FP is the number of positive labels classified as negative, and FN is the number of negative labels classified as positive.

- Precision: It determines the correctly predicted labels at TP and FP rates.

$$Precision = \frac{TP}{TP + FP} \quad (23)$$

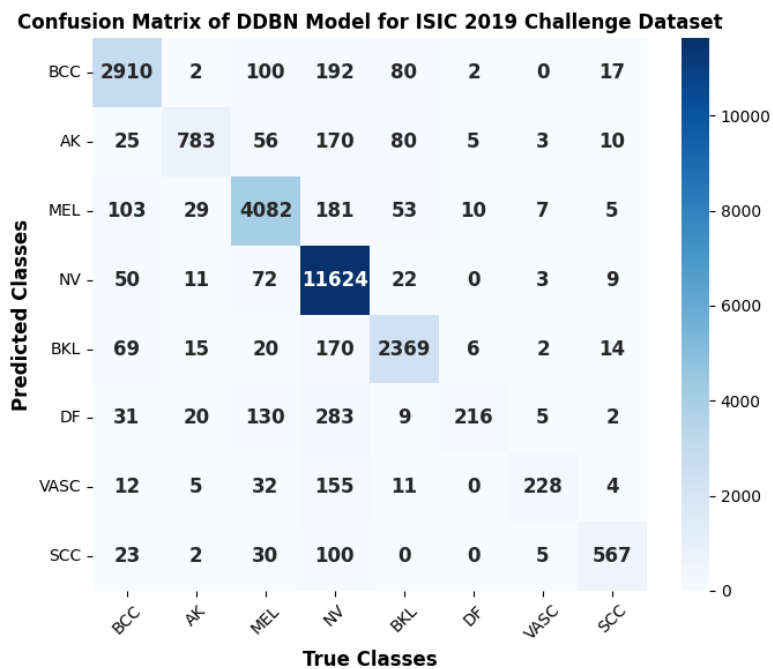
- Recall: It is the proportion of labels, which are correctly predicted at TP and FN rates.

$$Recall = \frac{TP}{TP + FN} \quad (24)$$

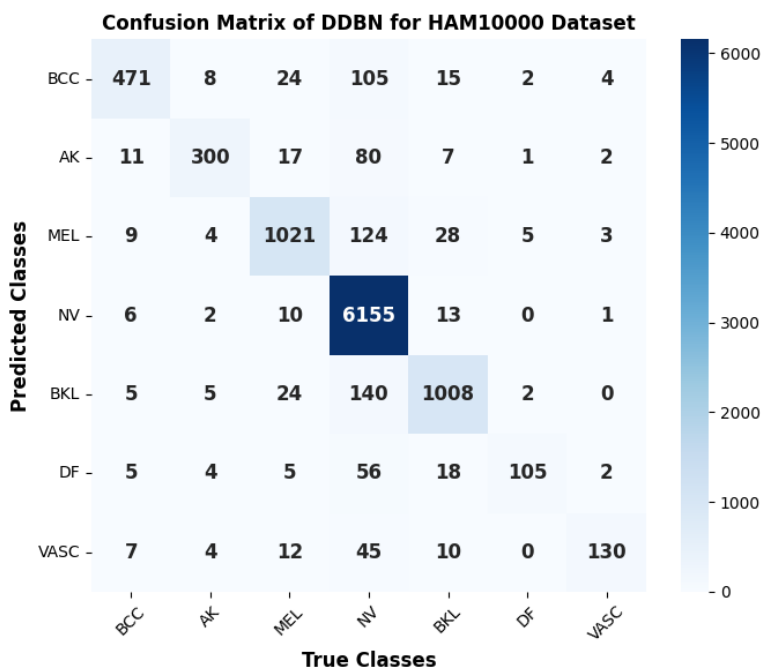
- F1-score (F1): It is the harmonic mean of precision and recall.

$$F1 = \frac{2 \times Precision \times Recall}{Precision + Recall} \quad (25)$$

The confusion matrix results for each class in the ISIC 2019 Challenge dataset and the HAM10000 dataset are shown in Figure 8 for the DDBN classifier.



(a)



(b)

**Figure 8. Confusion Matrix for DDBN Model. (a) ISIC 2019 Challenge Dataset and (b) HAM10000 Dataset**

Table 4 presents the overall classification performance for existing and proposed classifier models using the ISIC 2019 Challenge dataset and the HAM10000 dataset.



**Table 4. Performance Metrics of Proposed and Existing Models on Skin Image Datasets**

Dataset	Models	Precision	Recall	F1-score	Accuracy
		(%)			
ISIC 2019 Challenge	KNN	58.39	59.81	59.10	60.32
	SVM	72.64	73.28	72.96	74.05
	OP-DNN	86.15	86.43	86.79	86.85
	DDBN	89.42	89.19	89.31	90.28
HAM10000	KNN	66.92	67.14	67.03	67.27
	SVM	79.45	80.31	79.88	80.09
	OP-DNN	89.36	89.62	89.49	89.71
	DDBN	91.71	91.57	91.64	91.80

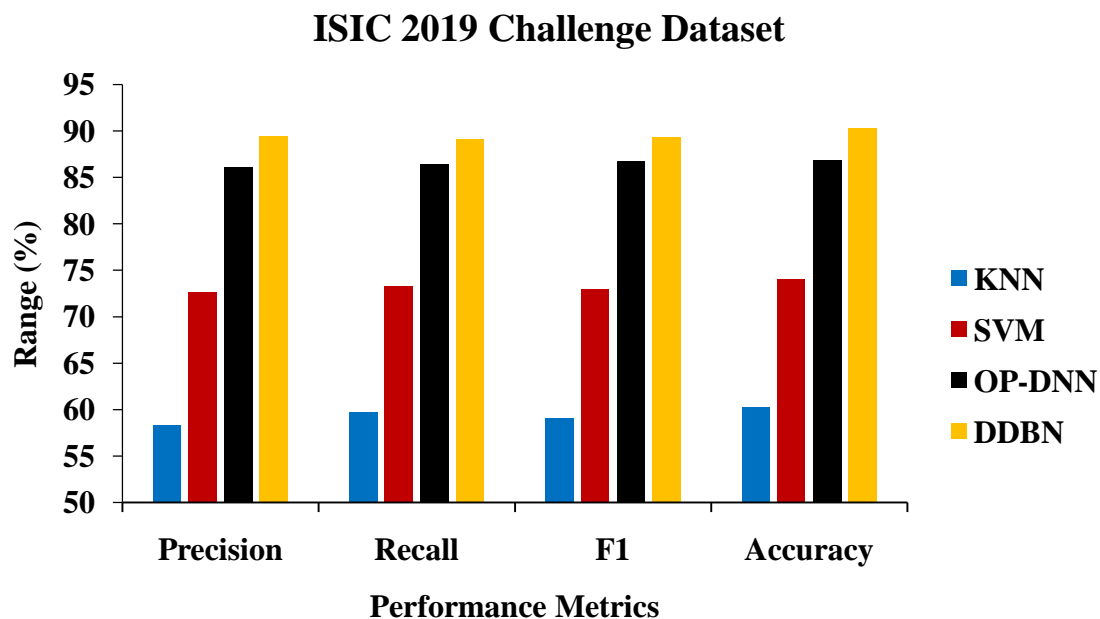
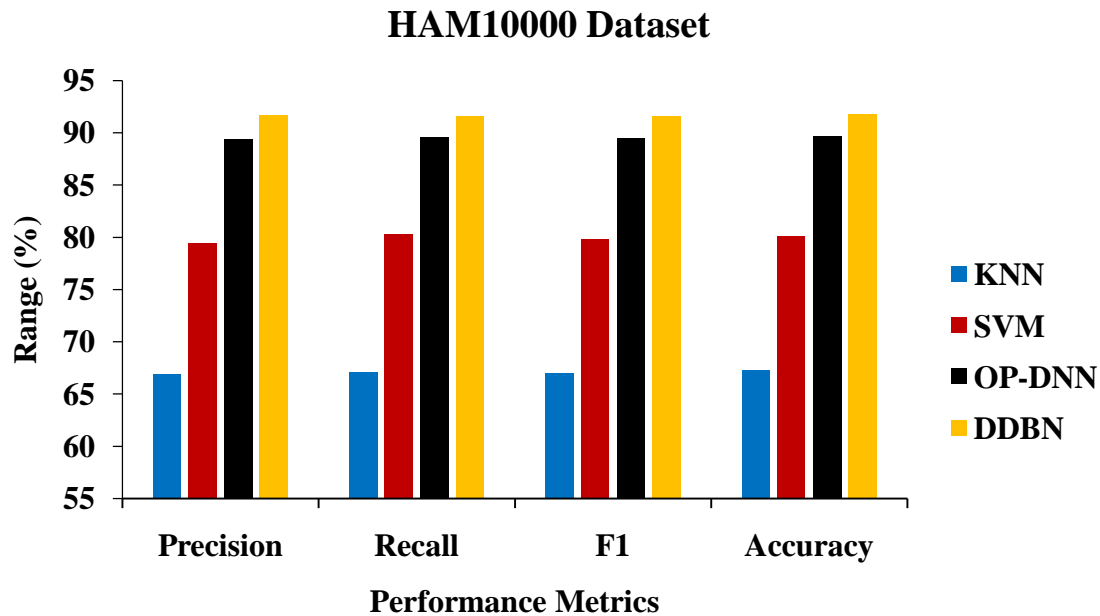
**Figure 9. Comparison of Different Skin Disease Classification Models on ISIC 2019 Challenge Dataset**

Figure 9 demonstrates the performance metrics of proposed and existing classification models on the ISIC 2019 Challenge dataset. It can be observed that the precision of DDBN classifier is 53.14%, 23.1% and 3.8% higher than the KNN, SVM and OP-DNN models, respectively. The recall is 49.12%, 21.71% and 3.19% higher than the KNN, SVM and OP-DNN models,

respectively. The F1-score is 51.12%, 22.41% and 2.9% higher than the KNN, SVM and OP-DNN models, respectively. Additionally, the accuracy is 49.67%, 21.92% and 3.95% higher than the KNN, SVM and OP-DNN models, respectively.



**Figure 10. Comparison of Different Skin Disease Classification Models on HAM10000 Dataset**

Figure 10 displays the performance metrics of proposed and existing classification models on the HAM10000 dataset. It can be observed that the precision of DDBN classifier is increased by 37.04%, 15.43% and 2.63% compared to the KNN, SVM and OP-DNN, respectively. The recall is increased by 36.39%, 14.02% and 2.18% compared to the KNN, SVM and OP-DNN models, respectively. The F1-score is increased by 36.71%, 14.72% and 2.4% compared to the KNN, SVM and OP-DNN models, respectively. Additionally, the accuracy is increased by 36.46%, 14.62% and 2.33% compared to the KNN, SVM and OP-DNN models, respectively.

## 4.1 Discussion

Key reasons behind the improved performance of the proposed DDBN model over existing models like SVM, KNN, and OP-DNN for skin disease classification include:

- **Effective preprocessing:** The proposed model employs preprocessing techniques to enhance the quality of skin images before further processing. This helps eliminate unwanted artifacts and noise that could negatively impact feature extraction and classification.
- **Accurate lesion segmentation:** The method utilizes the Mask-RCNN model to precisely identify and isolate lesion regions in skin images. Accurate lesion segmentation is crucial for extracting meaningful features.
- **Robust feature extraction:** This model extracts color and texture features from segmented lesion regions, including color moments and GLCM texture features. Combining color and texture information enhances the discriminative power of the feature set.
- **Deep learning capability:** DBNs are deep learning models composed of stacked RBMs that learn hierarchical representations of data. This capability is beneficial for complex tasks like skin disease diagnosis, where subtle variations in lesion characteristics are significant.

This leads to improved classification accuracy, precision, recall, and F1-scores compared to the existing models.

## V. CONCLUSION

This study introduces a new classifier, the DDBN model, for precisely classifying multiple skin diseases. It incorporates preprocessing, segmentation, feature extraction followed by the DDBN classifier for skin diseases classification. The performance of the DDBN model was evaluated on the ISIC 2019 Challenge and HAM10000 datasets, showing superior results compared to traditional classification methods like SVM, KNN, and OP-DNN. On the ISIC 2019 dataset, the DDBN achieved an accuracy of 90.28%, surpassing KNN (60.32%), SVM (74.05%), and OP-DNN (86.85%). Similarly, on the HAM10000 dataset, the DDBN achieved an accuracy of 91.80%, outperforming KNN (67.27%), SVM (80.09%), and OP-DNN (89.71%). This DDBN model can assist dermatologists and patients in the early and accurate detection skin diseases for

prompt intervention and treatment. Future research could explore incorporating additional clinical data and expanding the model to classify a wider range of skin conditions.

## REFERENCES

- [1] Hayat, S. N., &Indraswari, R. (2024). Skin cancer detection approach using convolutional neural network artificial intelligence. *International Journal of Informatics and Information Systems*, 7(2), 46-54.
- [2] Bonamonte, D., & Filoni, A. (2021). Impact of endocrine disorders on skin disorders. *Endocrinology and Systemic Diseases*, 399-434.
- [3] Kasolang, S., Adlina, W. A., Rahman, N. A., & Nik, N. R. (2020). Common skin disorders: a review. *JurnalTribologi*, 25, 59-82.
- [4] Kassem, M. A., Hosny, K. M., Damaševičius, R., &Eltoukhy, M. M. (2021). Machine learning and deep learning methods for skin lesion classification and diagnosis: a systematic review. *Diagnostics*, 11(8), 1390.
- [5] Adegun, A., &Viriri, S. (2021). Deep learning techniques for skin lesion analysis and melanoma cancer detection: a survey of state-of-the-art. *Artificial Intelligence Review*, 54(2), 811-841.
- [6] Bajwa, M. N., Muta, K., Malik, M. I., Siddiqui, S. A., Braun, S. A., Homey, B., ... & Ahmed, S. (2020). Computer-aided diagnosis of skin diseases using deep neural networks. *Applied Sciences*, 10(7), 2488.
- [7] Almuayqil, S. N., Abd El-Ghany, S., &Elmoghy, M. (2022). Computer-Aided diagnosis for early signs of skin diseases using multi types feature fusion based on a hybrid deep learning model. *Electronics*, 11(23), 4009.
- [8] Hameed, N., Shabut, A. M., Ghosh, M. K., & Hossain, M. A. (2020). Multi-class multi-level classification algorithm for skin lesions classification using machine learning techniques. *Expert Systems with Applications*, 141, 112961.
- [9] Sinthura, S. S., Sharon, K. R., Bhavani, G., Mounika, L., & Joshika, B. (2020). Advanced skin diseases diagnosis leveraging image processing. In *International Conference on Electronics and Sustainable Communication Systems*, pp. 440-444.
- [10] Jagdish, M., Guamangate, S. P. G., López, M. A. G., De La Cruz-Vargas, J. A., & Camacho, M. E. R. (2022). Advance study of skin diseases detection using image processing methods. *Natural Volatiles & Essential Oils Journal*,9(1), 997-1007.

- [11] Naeem, Z., Zia, G., & Bukhari, Z. (2022). A healthcare model to predict skin cancer using deep extreme machine learning. *Journal of NCBAE*, 1(2), 23-30.
- [12] AlDera, S. A., & Othman, M. T. B. (2022). A model for classification and diagnosis of skin disease using machine learning and image processing techniques. *International Journal of Advanced Computer Science and Applications*, 13(5), 252-259.
- [13] Hatem, M. Q. (2022). Skin lesion classification system using a K-nearest neighbor algorithm. *Visual Computing for Industry, Biomedicine, and Art*, 5(1), 7.
- [14] Maduranga, M. W. P., & Nandasena, D. (2022). Mobile-based skin disease diagnosis system using convolutional neural networks (CNN). *IJ Image Graphics Signal Process*, 3, 47-57.
- [15] Jain, A., Rao, A. C. S., Jain, P. K., & Abraham, A. (2022). Multi-type skin diseases classification using OP-DNN based feature extraction approach. *Multimedia Tools and Applications*, 1-26.
- [16] Sreekala, K., Rajkumar, N., Sugumar, R., Sagar, K. D., Shobarani, R., Krishnamoorthy, K. P., ... & Yeshitla, A. (2022). Skin diseases classification using hybrid ai based localization approach. *Computational Intelligence and Neuroscience*, 2022.
- [17] <https://challenge.isic-archive.com/data/#2019>
- [18] <https://www.kaggle.com/datasets/surajghuwalewala/ham1000-segmentation-and-classification>